



Research article

Unmanned aerial system protocol for quarry restoration and mineral extraction monitoring

Vicenç Carabassa^{a,b,*}, Pau Montero^{a,c}, Marc Crespo^{a,c}, Joan-Cristian Padró^c, Xavier Pons^c,
Jaume Balagué^d, Lluís Brotons^{a,d,e}, Josep Maria Alcañiz^{a,b}

^a CREAM, E08193, Bellaterra, Cerdanyola del Vallès, Catalonia, Spain

^b Universitat Autònoma de Barcelona, E08193, Bellaterra, Cerdanyola del Vallès, Catalonia, Spain

^c Grumets Research Group, Dep. Geografia, Edifici B, Universitat Autònoma de Barcelona, Bellaterra, 08193, Catalonia, Spain

^d Unitat Mixta InForest (CTFC-CREAM), Solsona, 25280, Spain

^e CSIC, Cerdanyola del Vallès, 08193, Spain



ARTICLE INFO

Keywords:

Drones
Open-pit mines restoration
Soil erosion
Photogrammetry
DSM
kNN classifier

ABSTRACT

Mining is an important activity of the primary sector with strong economic and environmental impacts. All over the world, governments have made efforts to regulate mine restoration by monitoring and assessing the evolution of mined sites. Our work aims to synthesize various remote sensing applications into a single workflow in order to obtain cartographic products using Unmanned Aerial Systems (UAS), not only for mine restoration management, but also as a way of monitoring mining activity as a whole. The workflow performs image processing and terrain analysis calculations, which conduct a supervised classification of the land cover. The resulting mapping products include orthoimagery, Digital Surface Models (DSM), land cover maps, volume variation calculations, dust deposition, detection of erosion problems, and drainage network evaluation maps. The data obtained from red-green-blue (RGB) sensors has a spatial resolution of 4–10 cm, providing information that allows the characterization of land covers with an overall accuracy of 91%. In comparison, if using multispectral sensors with the same flight conditions than RGB, image spatial resolution diminishes and land cover characterization accuracy drops to 81%. The resulting digital maps can be fully integrated into Geographic Information Systems (GIS), allowing the quantification of environmental features and spatial changes. Our study provides the basis for creating a large-scale, replicable and ready-to-use workflow suited for monitoring the exploitation of minerals and mine restoration using RGB imagery obtained through drones.

1. Introduction

Landscapes affected by human activity cover an increasing portion of the earth's surface, thereby significantly changing the pre-existing morphology (Lewin and Macklin, 2014; Tarolli and Sofia, 2016). In most countries, open-pit mines represent an economic pillar that provide raw materials for construction, public works and industrial sectors. In

addition, the growing demand for materials suggests that this activity will continue increasing until 2050 (Vidal et al., 2013).

The exploitation of open-pit mines affects the vegetation land cover, soil properties and hydrological structure (Osterkamp and Joseph, 2000). Among these effects, we can determine four large impact groups: erosion, subsidence, hazards and runoff (Xiang et al., 2018). Consequently, most natural landscapes affected by open-pit mines and other

Abbreviations: DEM, Digital Elevation Model; DHdM, Digital High differences Model; DIM, Digital Illumination Model; DMd, Digital Model Difference; DoD, Difference of Distances; DPC, Digital Point Cloud; DSdM, Digital Slope difference Model; DSM, Digital Surface Model; DTM, Digital Terrain Model; FAM, Flux Accumulation Model; GCP, Ground Control Point; GIS, Geographical Information System; GNSS, Global Navigation Satellite System; GPS, Global Positioning System; GRE, green (spectral region); HSI, Hue Saturation Intensity; kNN, k-Nearest Neighbor; MSAVI, Modified Soil Adjusted Vegetation Index; NdPD, Normalized difference Point Distance; NDVI, Normalized Difference Vegetation Index; NDWI, Normalized Difference Water Index; NIR, near-infrared (spectral region); RGB, red-green-blue (spectral region); REG, red edge (spectral region); ROI, Region Of Interest; RS, Remote Sensing; SAVI, Soil Adjusted Vegetation Index; SfM, Structure from Motion; SIFT, Scale-Invariant Feature Transform; TA, Training Area; TIN, Triangulated Irregular Network; UAS, Unmanned Aerial System; UAV, Unmanned Aerial Vehicle; VdM, Volume Difference Model; VNIR, visible and near-infrared (spectral region).

* Corresponding author. CREAM, E08193, Bellaterra, Cerdanyola del Vallès, Catalonia, Spain.

E-mail address: v.carabassa@creaf.uab.cat (V. Carabassa).

<https://doi.org/10.1016/j.jenvman.2020.110717>

Received 30 January 2020; Received in revised form 4 May 2020; Accepted 5 May 2020

Available online 20 June 2020

0301-4797/© 2020 The Authors. Published by Elsevier Ltd. This is an open access article under the CC BY license (<http://creativecommons.org/licenses/by/4.0/>).

highly disturbing activities (road construction, landfills) suffer very significant ecological impacts in terms of how these areas and their surroundings subsequently deteriorate (Carabassa et al., 2020; Chen et al., 2015). To prevent the degradation of these affected spaces, restoration measures need to be developed and implemented once activity ends (Carabassa et al., 2012, 2019). Restoration, monitoring and periodic inspection of these activities is required for the efficient management of natural resources, and is mandatory in most countries according to mine restoration legislation at different levels (European Directive 2006/21/EC, Spanish RD 975/2009, German Bundesberggesetz 1980, Catalan Law 12/1981). However, this monitoring is difficult to achieve through classic and time consuming in-situ methods (e.g. field transects and plots, floristic inventories, direct observations) by officials or involved companies and agencies. This is because of the huge surface area of some mines, the difficulty to access to some places, the risks associated with direct monitoring of some restored or active areas (e.g. close to extraction fronts or on steep slopes) and the lack of inspectors and funding available for this monitoring.

In this context, remote sensing systems offer direct and customizable monitoring and control capacity. Thus, they are powerful tools for agents involved in the management and recovery of exploited mines, and contribute towards minimizing the negative effects associated with mining activities (Karan et al., 2016; Hüttl and Weber, 2001). The study of open-pit mine monitoring has undergone a substantial change in recent years as a result of incorporating new technologies in place of traditional methods. Initially, this was with the introduction of satellite and aerial images which made it possible to monitor vegetation and exploitation in large areas (Lawley et al., 2016; OSMRE, 2015). However, the relatively low spatial resolution of satellite images, the high cost of taking images with airplanes or the constraints related to cloud conditions in both cases have led to the development of Unmanned Aerial Systems (UAS) or drones.

Previous experiences in monitoring restoration projects located in open-pit mines, with the aid of multispectral sensors, have yielded interesting results (Padró et al., 2019). As a result, the ability to map land cover in the study areas helps in subsequently evaluating the quality of the actions developed in restoration policies. However, multispectral UAS-sensors are not usually capable of obtaining similar spatial resolution to RGB, at the same flight height, since RGB have a resolution that is one order of magnitude higher. Moreover, in the context of areas of flight with steep slopes or vertical walls like those existing in quarries, low flight heights such as those required for multispectral cameras may not be possible for security and time lapse reasons, and are more time consuming.

Apart from land cover mapping, the study of point clouds derived from UAS flights also makes it possible to study relief changes, for instance, by differentiating the extraction and collection sites in the exploited areas (Xiang et al., 2018; Ruiz-Carulla et al., 2017), observing possible ground movements and their associated problems in restored areas (Cooke and Johnson, 2002), or specifically assessing vegetation changes (Vidal-Macua et al., 2020).

During the last decade, the use of UAS has become a popular and accessible technology for monitoring, modeling and mapping the terrain (Kandissounon et al., 2018; Manfreda et al., 2018). Through the Structure from Motion (SfM) techniques (Carrivick et al., 2016), it is now possible to obtain products with centimetric resolutions, i.e. orthophotoimages and Digital Terrain Models (DTM) including Digital Elevation Models (DEM) and Digital Surface Models (DSM). These algorithms allow the quick and easy spatial identification of common points in the images (Micheletti, 2015). The Scale-Invariant Feature Transform (SIFT) algorithm breaks down the image into a database of singular points. The points identified are invariant regardless of the image scale or rotations and are only slightly influenced by changes in illumination (Lowe, 2004).

The objective of our work is to propose a novel workflow for generating quantitative spatial information, focusing on restoration

failures and successes, in order to support private companies, public administration and environmental scientists in their use of UAS low-cost techniques for monitoring land restoration efforts not only during the exploitation phase of open-pit mines but also after cessation of mining activities. By using RGB imagery derived from UAS, the protocol focuses on analyzing and generating detailed cartography in a semi-automatic way to monitor key parameters, such as vegetation development and encroachment, soil erosion, drainage network evaluation and even dust deposition maps when present. The goal is to extract very detailed drone-derived digital data (sampling distances below 10 cm) to generate high resolution quantitative information useful to help decision making with objective indicators, and not biased by personal valuations. Results about the application of our protocol are presented and discussed, comparing RGB and multispectral data derived products.

2. Material and methods

2.1. Study area

The study has been carried out in three quarries located in Catalonia (NE Iberian Peninsula), which cover different restoration landforms, technosols and Mediterranean climates, from sub-humid to semi-arid (Fig. 1, Table 1, Map M1).

In all the areas studied, a variety of land covers has been included (herbaceous vegetation cover, shrubland, tree forest, eroded areas, mine wastes areas, bare soil, area affected by dust deposition, extraction fronts) in order to have a representative sample of the most relevant types existing in quarries. All the studied quarries produce calcareous aggregates, two of which were active when conducting the flights (Falconera and Pontils), while the other one was abandoned (Jornet). In active quarries, the revegetation approach consisted of the sowing and planting of a remarkable variety of species, which were intended to support the recovery of native species (Alcañiz et al., 2011). On the abandoned quarry, revegetation was spontaneous and no specific actions were carried out.

2.2. Systems and sensors

For the image-taking process, multi-engine aerial platforms, low-cost UAS of the brand DJI Phantom 3 Pro (DJI, 2015) in Pontils and Phantom 4 Pro (DJI, 2017) in Jornet were used. The optical sensor used for RGB data collection was the FC300X (Phantom 3 Pro) and CMOS '1 (Phantom 4 Pro). The sensor used for multispectral data collection was a Parrot Sequoia. This last sensor works with the bands G (Green), R (Red), Reg (Red Margin), NIR (Near Infrared) (Parrot Drones, 2016). The technical characteristics of the RGB and multispectral sensors used are indicated in Table S1.

2.3. Workflow

To carry out the study, the following protocol was proposed (Fig. 2). In the first place, the area of interest of each flight zone was identified and characterized to carry out the data collection. The acquisition of aerial photographs using UAS in both longitudinal and transversal orientations was performed with an overlap of 80%. The height of the flights was adapted to the altimetry of the terrain, programming the camera to trigger at different heights, from 60 m to 106 m. Applying such an adjustment allowed the minimization of the error associated with the topography variability in the area. With the images taken on the various flights, a digital photogrammetric reconstruction process was carried out using the specialized software Agisoft Photoscan (Agisoft, 2018). The image treatment (Micheletti, 2015) can also be carried out using appropriate software such as Visual SfM (Wu, 2013) or Pix4D (Pix4D, 2017).

During the digital photogrammetric reconstruction process, the starting images have position data from the scene center and can

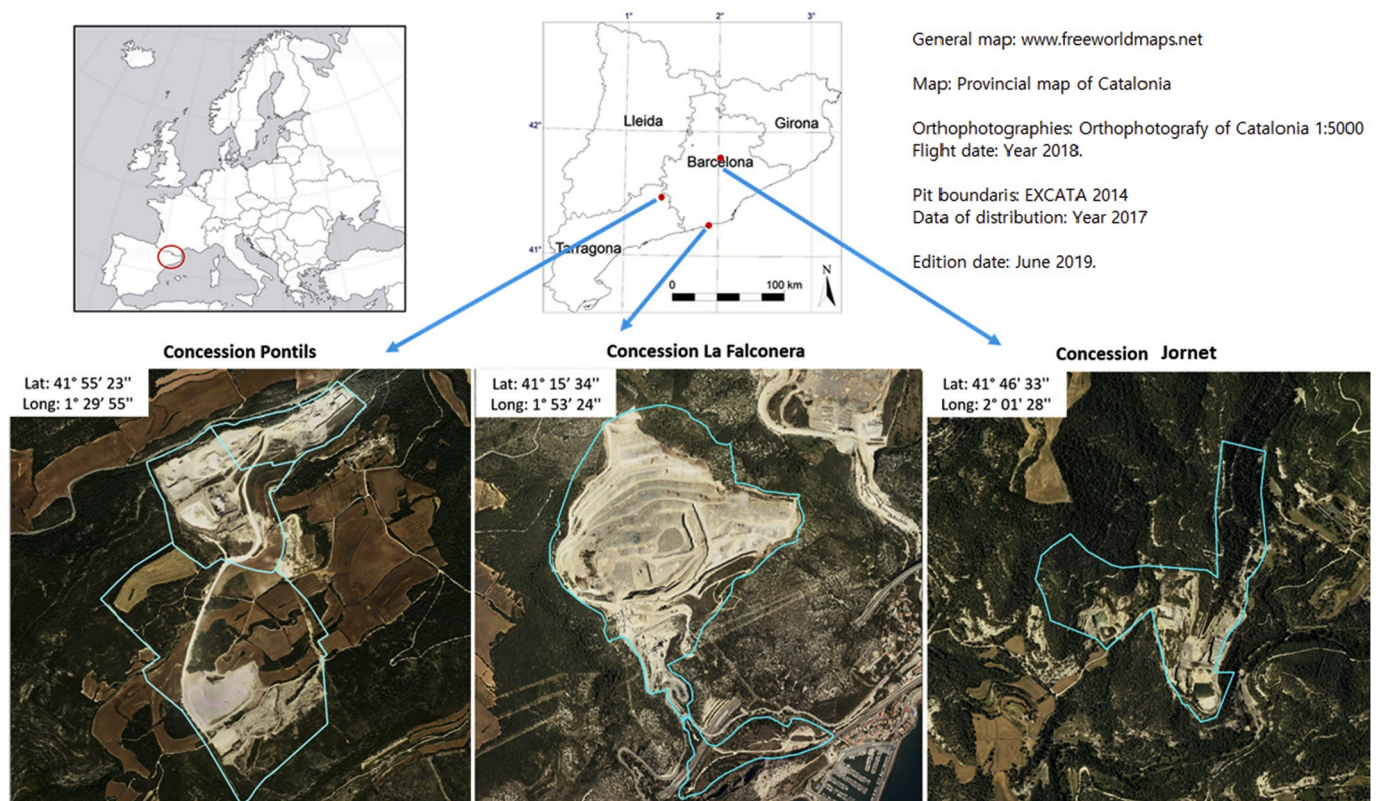


Fig. 1. Location and authorized exploitation limits (blue lines) of the three quarries included in this study (GENCAT, 2014), over the official regional agency orthophotomaps (ICGC, 2019). General map from www.freeworldmap.com. (For interpretation of the references to color in this figure legend, the reader is referred to the Web version of this article.)

therefore generate positions relative to the block of images as a whole. This process provides an agile and basic orientation that is subsequently completed by orienting the cameras in each of the acquisitions. Moreover, the images are compared in pairs in order to obtain homologous characteristic points through the SIFT process (Lowe, 2004). As a result, the software is able to reconstruct a 3D model of the surface photographed and can thus obtain a point-oriented cloud. Subsequently, the point cloud is densified and the orthomosaics of the surfaces of interest are obtained.

For the present study, control points were not used as these are only necessary in the multi-temporal analysis of earthworks or other comparative works. It is also possible to make a record of the images taken with the Sequoia (VNIR) and the UAS Phantom (RGB) sensors (Padró et al., 2019). After obtaining both the orientation of each scene

center at the time of the shooting, and a dense point cloud, a point cloud mesh was generated. This surface allowed us to generate an orthoimage from the aerial images.

After the photogrammetric processing, the resulting products were used in Remote Sensing (RS) and Geographical Information Systems (GIS) software, namely MiraMon (Pons, 2019) and QGIS (QGIS, 2020), which are specifically devoted to spatial analysis and have geostatistical capabilities. The statistical analyses and map mathematics were performed with different modules included in the referenced RS and GIS softwares, but the overall workflow can be applied using most similar commercial software.

Based on NdPD, non-morphological volumes such as trees and grey infrastructures were identified analyzing the changes in orientation of the normal points within a radius of interest (Fig. 3). This process also

Table 1

Quarry sites, their location, climatic conditions (precipitation and temperature), exploitation authorized area according to GENCAT (2014), and restoration characteristics (morphology, filler material and organic and mineral substrates used for Technosol construction, A and B horizons) and reference system (plant community of the surrounding area).

Site	Latitude (N)	Longitude (E)	Mean annual precipitation (mm)	Mean annual temperature (°C)	Exploitation authorized area (ha)	Landform	Technosol parental material (C horizon)	Technosol parental material (A horizon)	Reference ecosystem
Pontils	41° 55' 23''	1° 29' 55''	584	12.6	82	Terrace/berm embankment with steep slope	Rocky debris	Excavated soil	<i>Quercus faginea</i> and <i>Pinus nigra</i> forest
Falconera	41° 15' 40''	1° 53' 12''	545	15.5	79	Terrace/berm embankment with steep slope, flat areas	Excavated soil and mining wastes	Excavated soil and organic amendments	<i>Pinus halepensis</i> forest and mediterranean maquia
Jornet	41° 46' 33''	2° 01' 28''	669	13.1	38	Continuous slope with berms, flat areas	Geologic substrate (marl)	Geologic substrate (marl)	<i>Quercetum rotundifoliae typicum</i> with low forest

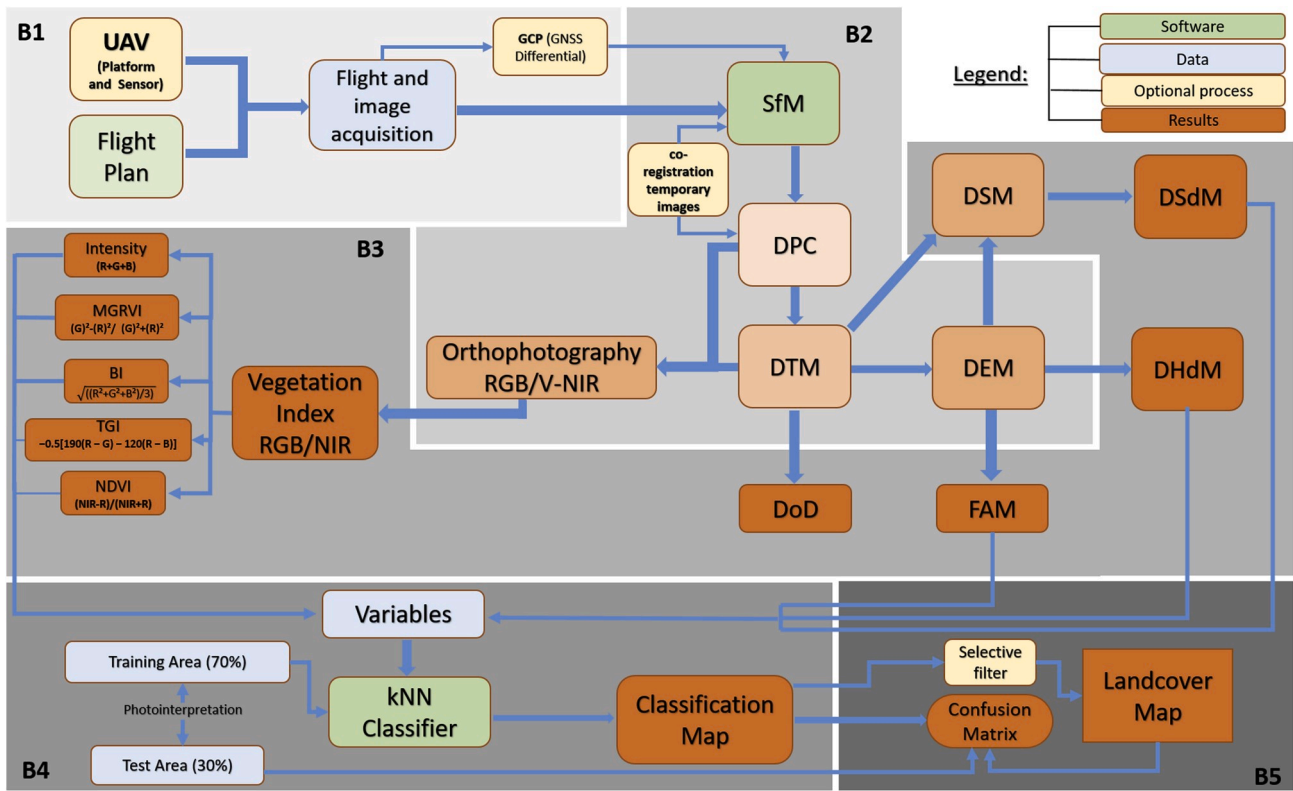


Fig. 2. Workflow for UAV use in monitoring exploitation and restoration in open-pit mines. UAV: Unmanned Aerial Vehicle; GCP: Ground Control Point; SfM: Structure from Motion; PC (Point Cloud); DSM (Digital Surface Model); DEM (Digital Elevation Model); DDM (Difference of Digital Models); FAM (Flow Accumulation Model); DHdM (Digital Height difference Model); DSM (Digital Slope difference Model).

allows us to create two typologies of digital models: the first typology provides information on the whole cloud of points (once it is cleared of noise and low points) corresponding to the DSM, and the second shows the points classified as a relief, representing the DEM.

With the aim of creating a cost-effective method, we studied the incorporation of various vegetation indices as a classification variable

(Table S2, Fig. 4). It has to be noted that each vegetation index based on RGB has certain strengths and limitations in terms of highlighting or omitting information on specific surfaces (McKinnon and Hoff, 2017). Therefore, it should be taken into account that the application of vegetation indices based on RGB is limited in regard to monitoring certain stages of vegetation growth (Bendig et al., 2015; Tucker, 1979).

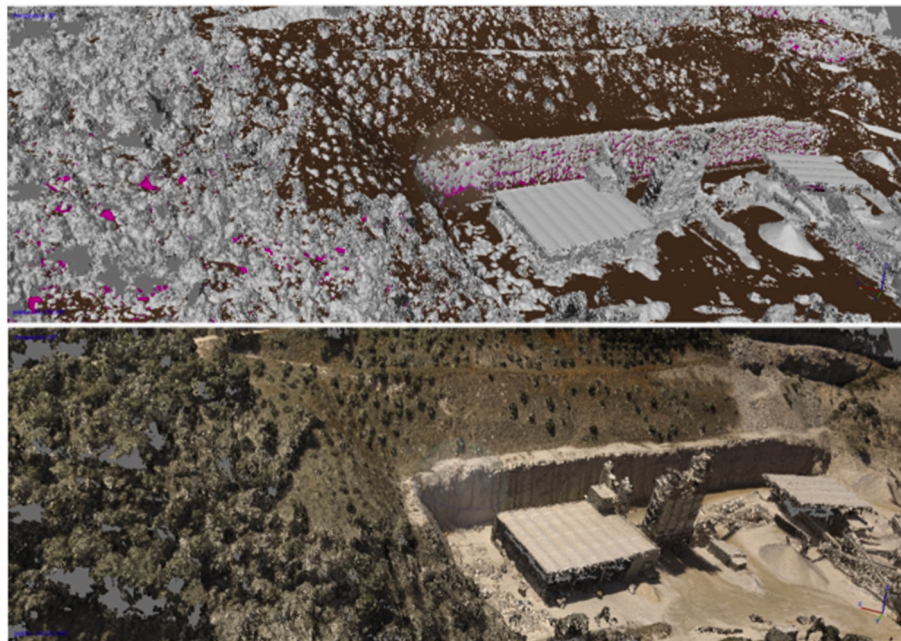


Fig. 3. Upper: Classified points (brown: ground; white: discriminated points; fuchsia: outliers). Bottom: Original point cloud. (For interpretation of the references to color in this figure legend, the reader is referred to the Web version of this article.)

The Modified Green Red Vegetation Index, MGRVI (Bendig et al., 2015), was derived from the Green Red Vegetation Index (Tucker, 1979), GRVI. The Triangular Greenness Index, TGI (Hunt et al., 2012), estimates the concentration of chlorophyll in leaves and land cover based on the analysis of green wavelength reflectance. In our work, the TGI index was used to determine the concentration of dust, generated by mineral extraction and processed, covering the woody vegetation canopy. The Brightness Index, BI (Mathieu et al., 1998), calculates the mean global reflectance of the spectral bands, and facilitates the detection of green covers (Mandal, 2016). On the other hand, the Normalized Difference Vegetation Index, NDVI (Rouse et al., 1974), was performed to compare the results obtained with the previous indices based on the visible spectrum. The NDVI is a widely known index that provides very good results in the spectral detection and discrimination of vegetation types. This is because it incorporates a spectral strip in the near infrared, yielding a high indication of the monitored area of vegetation. Finally, an index of intensities (RGB to HSI, space color transformation) was calculated in order to discriminate shadow areas. The result does not generate high values because the pixels that accumulate lower intensities are probably in shadowed areas. DHdM is a variable that is crucial for 3D data interpretation. DHdM is derived from the difference between the surface model and the elevation model (Bendig et al., 2013; Padró et al., 2019). DHdM contains information about the heights of the different objects (tree, scrub, building, etc.) that are identifiable in the landscape:

$$DHdM = DSM - DEM$$

Where DSM is the Digital Surface Model and DEM, the Digital Elevations Model.

Another variable, which can be obtained from the 3D cloud, is the model of the difference between slopes of the DSM and DEM (DSdM)

that informs us of the slope of each object. This model facilitates in discriminating the topographic slope from the slope between objects:

$$DSdM = SDM(HDDM)$$

An interesting and useful model in detecting streams and areas of preferential circulation of water in the terrain is the Flow Accumulation Model (FAM). Developed by Jenson and Domingue (1988) this type of algorithm tracks the path that a flow would have when sliding through the DEM until it finally leaves the digital model or ends in a sink or depression of the same model. To obtain the FAM, the SAGA GIS software (Conrad et al., 2015) was used. Depending on the type of geomorphology of the study area, one algorithm or another was applied: Rho 8 (Fairfield and Leymarie, 1991) or DEMON (Costa-Cabral and Burges, 1994).

The automatic classifier used was MiraMon's kNN (Nearest Neighbor) software (Pons, 2004). This supervised classifier assumes that the pixels that are united in the statistical space belong to the same informative class, i.e. it classifies a pixel by examining the available information pixels in the statistical space and choosing the most represented informative class in the set of neighbors that are in the vicinity. A Euclidean distance in the multivariate statistical space was used for this purpose. Training areas were defined by in situ identification and photointerpretation of the different land covers with the help of the high-resolution orthoimages generated. In this case, the number of samples used to define classes is relevant at the time of using the kNN classifier. All cover categories had a similar total training area and also a similar number of polygons, with a total area for each category between 0.10% and 0.05% of the total mapped area. Moreover, training areas were distributed homogeneously covering all of the studied surface. The different categories proposed for the classification of the different land covers to be analyzed are described in Table 2.

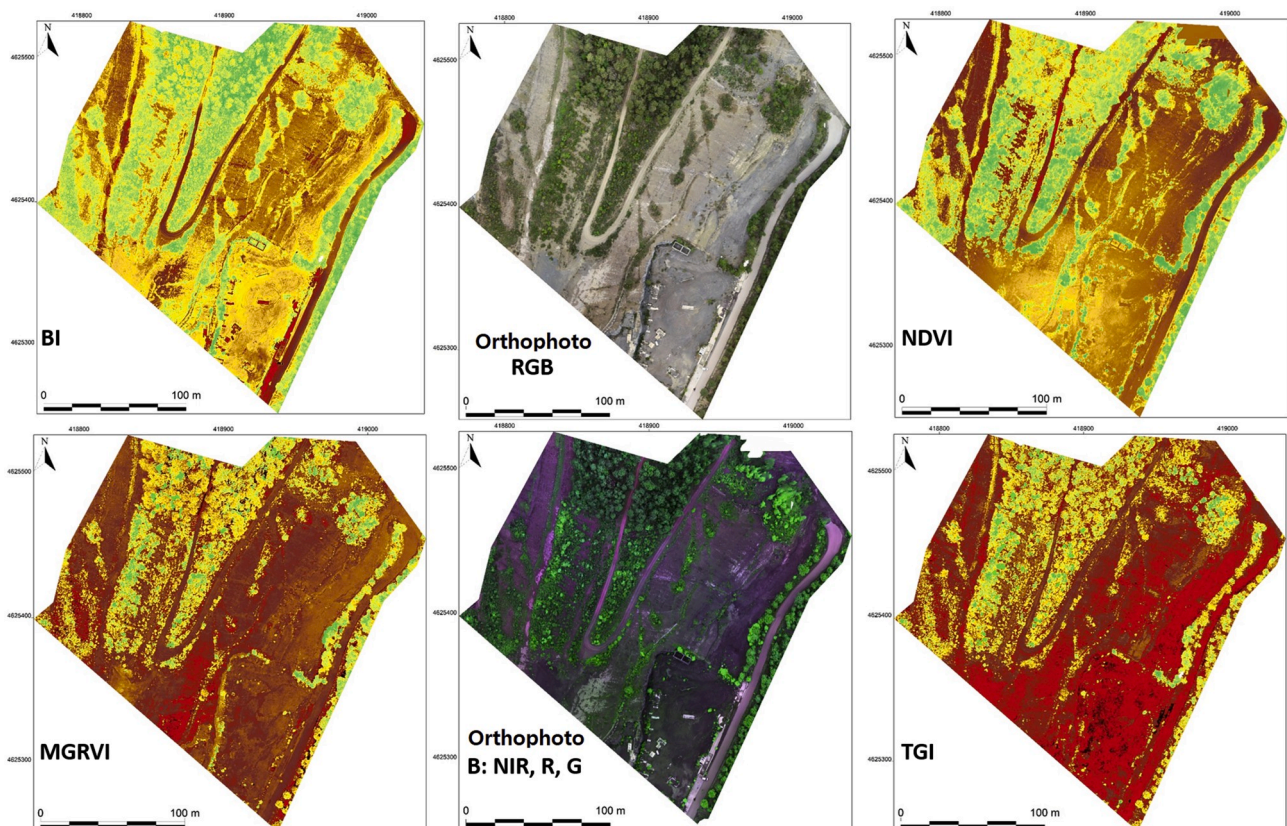


Fig. 4. Vegetation indexes based on RGB (MGRVI, BI, TGI) and on multispectral imagery (NDVI), orthophotoimage RGB and orthophotoimage false color for Jornet quarry. (For interpretation of the references to color in this figure legend, the reader is referred to the Web version of this article.)

Table 2
Categories proposed for the classification of land covers in open-pit mine restored areas.

Category	Description
Grass	Areas covered by grasslands and grasslands with presence of low grass
Shrubland	Woody species with a height less than 2 m. It can include both shrub and tree plants in early growth stages.
Tree	Woody species with a height greater than 2 m. It is mostly composed of trees and some high-rise shrub
Bare soil	Areas without vegetation cover and with a soil rich in organic matter (>2%)
Mining waste	Areas without vegetation cover and with a soil poor in organic matter (<2%)
Shadow	Areas where it is not possible to detect the cover due to the low intensity of the electromagnetic reflection captured by the sensor, this class is generated to avoid overestimating or underestimating the state of the covers.

For the classification of the different land covers in Pontils, the following variables were used: DHdM, MGRVI, DSdM, Intensity index. All variables were standardized while the DHdM variable was not normalized, thus maintaining the height data of landscape objects. For the classification of different soil covers in Jornet, the following variables were used: HddM, FAM, MGRVI, BI and DSdM. As in the previous case, the DHdM variable was not normalized.

As a final step, selective filtering was performed to reduce any “salt and pepper” effect. This process eliminates those sets of pixels with an area size smaller than desired. The surface was determined after assessing the size of the elements to be classified. It is recommended to eliminate areas smaller than 10 cm². To perform this step, we vectorized the land cover map and then selected those polygons that we wanted to remove. With this approach, the geometry of the polygon is not modified, as in the case of a common filter.

Confusion matrices were used to observe and determine the accuracy of the land cover map. These were created with truth-terrain areas, which we refer to as test areas. Using confusion matrices facilitated the detection and quantification of wrongly classified covers. Moreover, by studying the confusion matrices, it was possible to detect the classes that present the greatest error and with which covers they are confused.

Analyzing changes in exploitation fronts, stockpiles and mining dumps in the quarries can also provide additional information for mine management and restoration. In this study, we use time series derived from flights above La Falconera to calculate the volume changes. For these calculations, we decided to work with the point clouds and the M3C2 method (Lague et al., 2013) by means of the Cloud Compare software (CloudCompare 2.8.1, 2019). Although this method presents results in an agile and coherent way, the treatment of the results to generate a report of moved volumes required the rasterization of the result file or the usage of other volume calculation tools. For this purpose, the Volume 2.5D tool was used (CloudCompare 2.8.1, 2019), which rasterizes the point cloud to later perform a calculation between the generated rasters. The result obtained should again be treated in raster format to integrate the results generated in the study as a whole.

Since the previous method requires several formatting changes, a new workflow was performed without the point clouds, exclusively working with raster files. First, a Difference of Digital Models (DMd) of the range of interest was obtained. After, by knowing the area of the pixels, the cubic volume formula was applied to estimate the volume measures. Thus, the pixel area was applied as a multiplier factor to the DMd in order to obtain a Volume Difference Model (VdM) of the time interval being studied.

3. Results

3.1. Boundaries of authorized exploitation

One of the first products obtained by applying the described workflow are orthoimages with very high resolution (4–10 cm spatial resolution), which facilitate the evaluation of some aspects directly by means of photointerpretation. One of these aspects concerns the control of boundaries, as it is relatively easy to detect areas affected by extraction or preparation for extraction (vegetation clearing) outside of authorized limits, superposing the orthoimages generated to the boundaries layer in a GIS. In the Pontils quarry, an extra-limits area of 2800 m² has been detected by photointerpreting the high-resolution orthophotoimages generated (Fig. 5). This area was affected by extraction works a decade before the conducted flight, despite being out of the extraction authorized limits. At the time of the conducted flight, the monitored area was in the first stages of the restoration process, mainly dominated by herbaceous vegetation and with some planted seedlings growing (undergoing restoration). For this reason, the vegetation cover was clearly different from untouched areas (pine forest cover), for which it could be precisely delimited.

3.2. Land cover classification

For the recovery assessment of a study area, land cover classification is essential, in order to know which vegetation dominates and how the processes of encroachment and autochthonous vegetation recruitment are progressing. To carry out this assessment it is necessary to analyze in detail the variables that participate in the classification. It is observed for this case (AE Jornet) that the indices which offer the best response are MGRVI and BI. However, for the case of Pontils only MGRVI has been used (see Tables S3 and S4).

The visual result of the classification was consistent with the original images and the verifications carried out in the field for both case studies (Fig. 6, Map M2). In the case of Pontils, the shadow class presented a high commission error, significantly affecting the overall result of the classification that had a global accuracy of 90.64% (Table S6). It also presented difficulties in the process of discriminating organic and non-organic soil types with errors of commission and omission between both classes. In the multispectral classification, the shadow commission error was maintained and even increased, and therefore generally presented a weak result with a global accuracy of 81.00% (Table S4).

For RGB classification in Jornet, the shrubland class presented a high commission error that moderately affected the overall result of the classification. However, the other land covers were properly detected and presented a consistent result. Despite the error shown in the shrubland class a global accuracy of 85.38% was obtained (Table S7). Otherwise the multispectral classification presented difficulties when discriminating the shrubland and grassland classes; moreover, it presented a weaker result with a global success of 75.60% (Table S8).

3.3. Temporal study of earthwork movements

In the quantification of the volumes of materials moved (rocks, mining waste, aggregates, topsoil, etc.), results that respond to the changes detected are obtained by multitemporal drone flight. To obtain these results, a correct registration of the point clouds of the different flights is essential. In our case, georeferencing between flights was done by ground control points. For the monitoring of fronts, debris and storage, both data processing in point clouds and rasters offered very similar volumetric results. This data was obtained by using RGB images. This product served as the basis for detecting the active areas of the

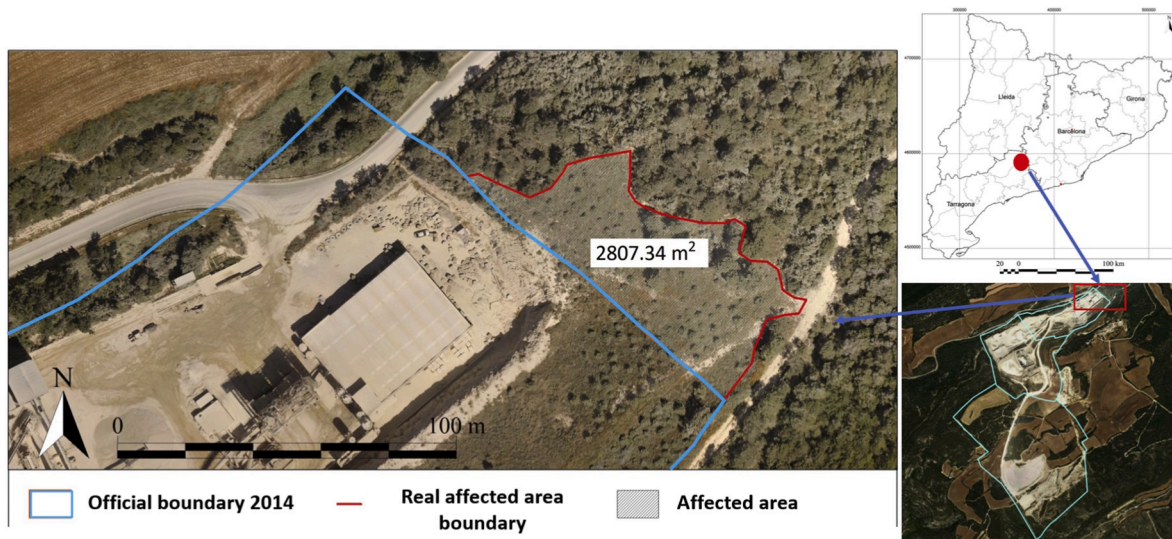


Fig. 5. Area located outside Pontils concession limits, determined through photointerpretation of the orthophotoimage RGB taken with UAV.

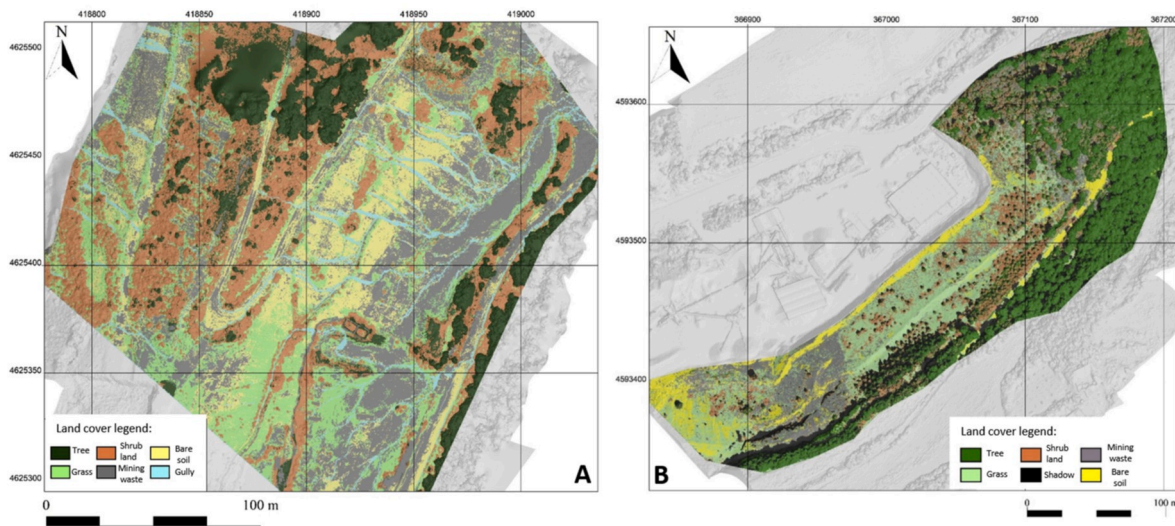


Fig. 6. Land cover classification for Jornet (A) and Pontils (B) restored areas.

quarries being monitored. Moreover, it could be used as a measure of evidence to provide justification for penalizing any extraction activities conducted in closed areas outside the operating limits or below the permitted topographical elevation. With this product, it is possible to estimate the volumes extracted from specific areas or specific slopes or from blasting (Fig. 7).

3.4. Gully detection

The technique of gully detection was carried out by implementing the FAM as another variable in the cover classification. For the case study, the FAM of Jornet is presented, which shows the classification of the cover gully. Moreover, the FAM could also help in evaluating the drainage web, by detecting breaks in evacuation channels (Fig. 8). That can be very useful to locate the points to be repaired and achieve effective erosion control.

3.5. Effects of dust deposition

To evaluate the impact of extractive activities on the nearby environment, the spectral signal of the vegetation covers were analyzed to

determine dust deposition. This data was obtained from the TGI index, as indicated in the methods section. In the northern area of the Pontils quarry, we observed a large area affected by dust deposition that we also observed in the RGB composition (Fig. 9). However, only the areas classified as woody vegetation were evaluated. Herbaceous decks were discarded from the analysis, given the similarity with non-vegetative ones, in terms of their relative height close to 0 m in the HdDM.

4. Discussion

The results obtained in this study confirm the possibility of making land cover classifications by using both a multispectral camera and a camera with RGB sensor in the visible. The methodology presented is developed with the objective of obtaining classifications in the visible spectrum, giving high importance to morphometric variables (DHdM, DSdM, FAM) in the process. However, the weight of these variables makes it difficult to distinguish shrub species from low-bearing trees.

Obtaining automatic classifications at the high spatial resolution of this work supposes a clear advantage compared to previous and recent work carried out in the context of mines, that are based on evaluating vegetation vigor directly through NDVI or similar vegetation indices

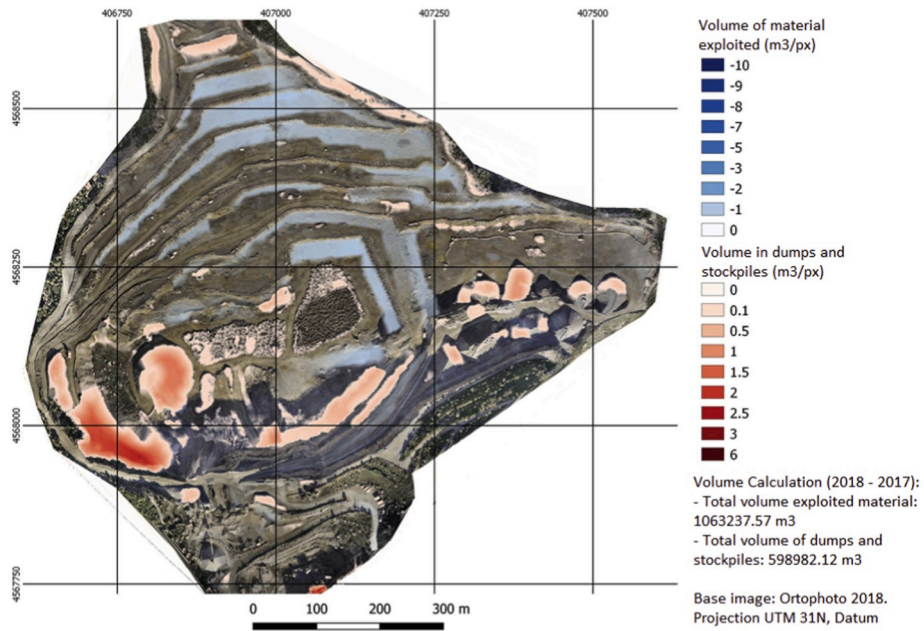


Fig. 7. Volumes extracted and accumulated in Falconera between 2017 and 2018. Total volume of material extracted: 1,063,237 m³. Total volume of debris and stockpiles: 598982 m³. Background image: Orthophoto 2018.

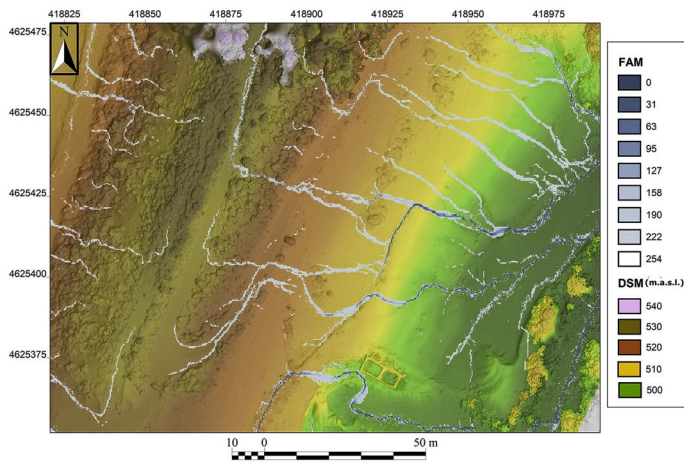


Fig. 8. Rill and gully map obtained through MAF in Jornet quarry, represented on DSM (a), details of drainage network affections (b), and heavy erosion problems (c).

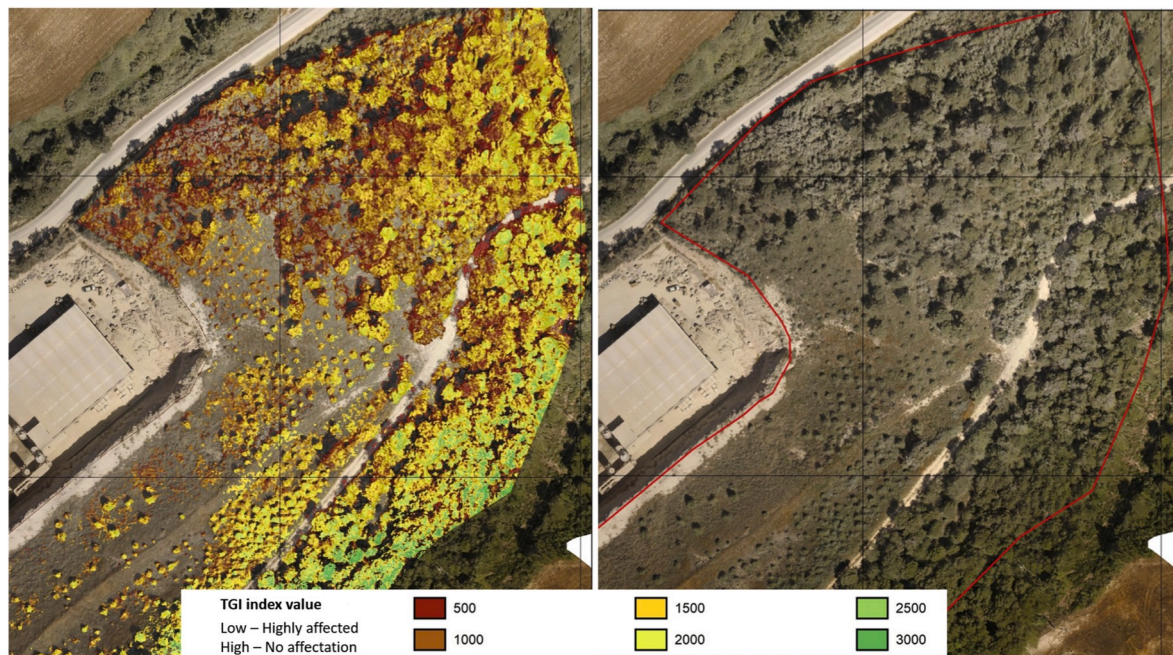


Fig. 9. TGI applied to woody vegetation in the restored area of Pontils quarry.

(Vidal-Macua et al., 2020; Bonifazi et al., 2003), without discriminating between vegetation types. Taking into account the principles of ecological restoration (Gann et al., 2019), basing restoration monitoring only on vegetation vigor will not give a proper idea of vegetation development in restored areas, especially when restoration actions have been carried out several years before and vegetation has been properly progressing.

Moreover, the global success values and Kappa indices obtained in the RGB classifications have higher values than those obtained with multispectral sensors. Regarding this, similar or better global success ratios and Kappa indices have been obtained using the RGB classifications obtained in the present work, than with the results obtained in recent and previous works (Padró et al., 2019; Zhang et al., 2019), despite using lower spectral resolution sensors (RGB). This result was due to the higher spatial resolution of the RGB cameras in the study. Resolution in pixel size is an important feature (Zhang et al., 2019; Addink et al., 2013), since usually sensors with bands in the infrared spectrum have weaker spatial resolution than RGB-sensors used in this study. The models derived from the DSM and DEM present greater detail with an RGB sensor, since these provide a better result in photogrammetric reconstruction. These results show a clear improvement compared to previous reconstructions obtained by the same team in the same context (Padró et al., 2019).

In general, the classification obtained offers satisfactory results, especially on woody covers larger or smaller than 2 m. Among these, some confusion arises when the height of the classified elements is close to 2 m because this type of vegetation (bushes and small trees) does not maintain a constant height due to their irregular growing type. Also, a successful result was obtained in the classification of the category of “gully”. Altogether, the promising results gained from this classification provide a good incentive for continuing to work with this type of variable (FAM).

In our study, we observed a greater salt and pepper effect in the classification obtained by the visible RGB sensor, while, for the map obtained by multispectral variables, the salt and pepper effect was not so noticeable. This is due to the fact that the spatial resolution in the visible RGB sensor is greater and, therefore, it presents greater noise (Hirayama et al., 2018). Note that this is an important issue when working with high spatial resolution imagery, including multispectral images (Padró

et al., 2019).

The visible RGB sensor presents confusion between the soil and grassland categories, since the latter category can present very similar values in the set of variables in the soil category, especially when the vegetation is dry. For a good classification, it is recommended to make the flights in the spring or early summer seasons (Padró et al., 2019), when the herb vegetation type has quite differentiated values compared to the organic soil or mining residue.

The presence of dust on the leaves of trees and shrubs was not detected using infrared bands. However, it is possible to detect this anomaly using the visible bands. RGB indices based on the green channel, such as TGI, offer a very good variable to assess the state of health of the flora given the sensitivity they present when detecting dust particles on plant surfaces (Hunt et al., 2012).

It is recommended to always take the images in the same period of the year, with spring and early summer being the best times, given the presence of green and active leaves in the monitored vegetation. Dawn and cloudy days are optimal conditions for imaging, since the effect of shadows is minimized, and diffuse radiation is available. For this purpose, it could be interesting to take images at solar noon (when the sun is at its zenith) in order to minimize shadows. For this reason, the images of La Falconera have not been classified, as a large part of the restored surfaces was in the shadowed area, since the images were captured during the morning and winter season.

The use of landmarks or features of the landscape, which are fixed and visible at the working scale, is recommended for the co-comparison between multi-temporal data or between the RGB and the sequoia (NIR) sensors. Also for the calculation of volume changes, it is highly recommended to use control points located in unvarying terrain or at the border of the authorized perimeter for a correct estimation of the volumes (Esposito et al., 2017).

5. Conclusions

The workflow presented allows the precise monitoring of mine extraction and restoration works, using ready to use, fast and low-cost technology. A UAS-based protocol allows fast monitoring of large and remote areas that would be impossible to monitor using classical field techniques, in order to obtain more precise and representative products.

The ability to classify land cover using RGB images helps to reduce the cost of the process obtaining higher quality products than using multi-spectral data, since RGB sensors usually have higher spatial resolution and a lower price. Automatic classification allows a reduction in photointerpretation work and increases the accuracy of the derived products (to >90%), although this could be validated and improved further by photointerpretation. The workflow is highly automatized through batch processes, but a specialized technician should be in charge of the process since the digitalization of training and validation areas is mandatory.

The interest of these applications will increase when time-series, that provide previous information, are available to compare with. In this sense, new products could be obtained like soil losses by erosion or vegetation change maps. This may increase the amount of monitoring and general scientific interest, since ecological and hydrological processes could be studied in high detail and covering large areas. Moreover, if needed, the workflow could be improved by incorporating other products like those related to geotechnical risks or plague infestation, amongst others.

Implementing this proposed workflow provides great potential on a large scale for effectively monitoring land restoration, as it can be used as a concrete tool for optimizing resources, ensuring sustainable measures for land restoration, as well as creating and strengthening synergies between companies, environmental scientists and public administrations.

Declaration of competing interest

The authors declare that they have no known competing financial interests or personal relationships that could have appeared to influence the work reported in this paper.

CRedit authorship contribution statement

Vicenç Carabassa: Conceptualization, Methodology, Validation, Investigation, Writing - original draft, Supervision, Project administration, Funding acquisition. **Pau Montero:** Software, Methodology, Validation, Formal analysis, Investigation, Writing - original draft. **Marc Crespo:** Software, Methodology, Validation, Formal analysis, Writing - original draft. **Joan-Cristian Padró:** Conceptualization, Software, Methodology, Formal analysis, Validation, Investigation, Writing - original draft, Supervision. **Xavier Pons:** Funding acquisition. **Jaume Balagué:** Investigation. **Lluís Brotons:** Writing - review & editing, Funding acquisition. **Josep Maria Alcañiz:** Conceptualization, Validation, Investigation, Writing - review & editing, Supervision, Project administration, Funding acquisition.

Acknowledgments

The authors would like to thank the support received by the project "Research and innovation in the process and control of the restoration of extractive activities", funded by the Department of Territory and Sustainability of the Government of Catalonia. This work has been partially funded by the Spanish MCIU Ministry through the NEWFORLAND research project (RTI2018-099397-B-C21 MCIU/AEI/ERDF, EU) and by the Government of Catalonia (SGR2017-1690, SGR2017-1569). Xavier Pons is a recipient of the ICREA Academia Excellence in Research Grant (2016–2020). We also express our gratitude to the RPAS Unit of the Rural Agents of the Government of Catalonia for the transfer of the images of Jornet quarry. Finally, we thank the company PROMSA (Ciments Molins) for the transfer of point clouds from La Falconera quarry.

Appendix A. Supplementary data

Supplementary data related to this article can be found at <https://doi.org/10.1016/j.jenvman.2020.110717>.

References

- Agisoft, 2018. *Agisoft PhotoScan Professional User Manual* 1–121.
- Bendig, J., Bolten, A., Bareth, G., 2013. UAV-based Imaging for Multi-Temporal, very High Resolution Crop Surface Models to monitor Crop Growth Variability—Monitoring des Pflanzenwachstums mit Hilfe multitemporaler und hoch auflösender Oberflächenmodelle von Getreidebeständen auf Basis von Bil. *Photogramm. Fernerkund. Geoinf.* 2013, 551–562. <https://doi.org/10.1127/1432-8364/2013/0200>.
- Bonifazi, G., Cutaia, L., Massacci, P., Roselli, I., 2003. Monitoring of abandoned quarries by remote sensing and in situ surveying. *Ecol. Model.* 170, 213–218. [https://doi.org/10.1016/S0304-3800\(03\)00228-X](https://doi.org/10.1016/S0304-3800(03)00228-X).
- Carabassa, V., Ortiz, O., Alcañiz, J.M., 2019. RESTOQUARRY: indicators for self-evaluation of ecological restoration in open-pit mines. *Ecol. Indic.* <https://doi.org/10.1016/j.ecolind.2019.03.001>.
- Carabassa, V., Domene, X., Alcañiz, J.M., 2020. Soil restoration using compost-like-outputs and digestates from non-source-separated urban waste as organic amendments: limitations and opportunities. *J. Environ. Manag.* 255 <https://doi.org/10.1016/j.jenvman.2019.109909>.
- Chen, J., Li, K., Chang, K.J., Sofia, G., Tarolli, P., 2015. Open-pit mining geomorphic feature characterisation. *Int. J. Appl. Earth Obs. Geoinf.* 42, 76–86. <https://doi.org/10.1016/j.jag.2015.05.001>.
- CloudCompare 2.8.1, 2019. CloudCompare (version 2.8.1) [GPL software]. Retrieved from <http://www.cloudcompare.org/>.
- Conrad, O., Bechtel, B., Bock, M., Dietrich, H., Fischer, E., Gerlitz, L., Wehberg, J., Wichmann, V., Böhner, J., 2015. System for automated geoscientific analyses (SAGA) v. 2.1.4. *Geosci. Model Dev* 8, 1991–2007. <https://doi.org/10.5194/gmd-8-1991-2015>.
- Cooke, J.A., Johnson, M.S., 2002. Ecological restoration of land with particular reference to the mining of metals and industrial minerals: a review of theory and practice. *Environ. Rev.* 10, 41–71. <https://doi.org/10.1139/a01-014>.
- Costa-Cabral, M.C., Burges, S.J., 1994. Digital Elevation Model Networks (DEMON): A model of flow over hillslopes for computation of contributing and dispersal areas. *Water Resour. Res.* <https://doi.org/10.1029/93WR03512>.
- DJI, 2015. Phantom 3 Pro - Users Manual. DJI.
- DJI, 2017. Phantom 4 Pro - Users Manual. DJI.
- Esposito, G., Mastrorocco, G., Salvini, R., Olivetti, M., Starita, P., 2017. Application of UAV photogrammetry for the multi-temporal estimation of surface extent and volumetric excavation in the Sa Pigada Bianca open-pit mine, Sardinia, Italy. *Environ. Earth Sci.* <https://doi.org/10.1007/s12665-017-6409-z>.
- Fairfield, J., Leymarie, P., 1991. Drainage networks from grid digital elevation models. *Water Resour. Res.* 27, 709–717.
- Gann, G.D., McDonald, T., Walder, B., Aronson, J., Nelson, C.R., Jonson, J., Hallett, J.G., Eisenberg, C., Guariguata, M.R., Liu, J., Hua, F., Echeverría, C., Gonzales, E., Shaw, N., Decler, K., Dixon, K.W., 2019. International Principles and Standards for the Practice of Ecological Restoration, second ed. *Restor. Ecol.* <https://doi.org/10.1111/rec.13035>.
- GENCAT, 2014. Generalitat de Catalunya (Departament de Territori i Sostenibilitat). Focus emissors al medi. *Activitats extractives*. http://territori.gencat.cat/ca/01_departament/12_cartografia_i_toponimia/bases_cartografiques/medi_ambient_i_sostenibilitat/bases_miramon/focus/04/.
- Hüttel, R.F., Weber, E., 2001. Forest ecosystem development in post-mining landscapes: a case study of the Lusatian lignite district. *Naturwissenschaften* 88, 322–329. <https://doi.org/10.1007/s001140100241>.
- ICGC, 2019. Institut Cartogràfic i Geològic de Catalunya, Vissir3. <http://www.icc.cat/vissir3/>.
- Jenson, S.K., Domingue, J.O., 1988. Extracting topographic structure from digital elevation data for geographic information system Analysis. *Photogramm. Eng. Rem. Sens.* 54, 1593–1600.
- Karan, S.K., Samadder, S.R., Maiti, S.K., 2016. Assessment of the capability of remote sensing and GIS techniques for monitoring reclamation success in coal mine degraded lands. *J. Environ. Manag.* 182, 272–283. <https://doi.org/10.1016/j.jenvman.2016.07.070>.
- Lague, D., Brodu, N., Leroux, J., 2013. Accurate 3D comparison of complex topography with terrestrial laser scanner: application to the Rangitikei canyon (N-Z). *ISPRS J. Photogrammetry Remote Sens.* 82, 10–26. <https://doi.org/10.1016/j.isprsjprs.2013.04.009>.
- Lawley, V., Lewis, M., Clarke, K., Ostendorf, B., 2016. Site-based and remote sensing methods for monitoring indicators of vegetation condition: an Australian review. *Ecol. Indic.* 60, 1273–1283. <https://doi.org/10.1016/j.ecolind.2015.03.021>.
- Lewin, J., Macklin, M.G., 2014. Marking time in Geomorphology: should we try to formalise an Anthropocene definition? *Earth Surf. Process. Landforms* 39, 133–137. <https://doi.org/10.1002/esp.3484>.
- Mandal, U.K., 2016. Spectral color indices based geospatial modeling of soil organic matter in Chitwan District, Nepal. *Int. Arch. Photogramm. Remote Sens. Spat. Inf. Sci. - ISPRS Arch.* 41, 43–48. <https://doi.org/10.5194/isprsarchives-XLI-B2-43-2016>.
- Manfreda, S., McCabe, M.F., Miller, P.E., Lucas, R., Madrigal, V.P., Mallinis, G., Dor, E., Ben, Helman, D., Estes, L., Ciruolo, G., Müllerová, J., Tauro, F., de Lima, M.I., de Lima, J.L.M.P., Maltese, A., Frances, F., Caylor, K., Kohv, M., Perks, M., Ruiz-Pérez, G., Su, Z., Vico, G., Toth, B., 2018. On the use of unmanned aerial systems for environmental monitoring. *Rem. Sens.* 10 <https://doi.org/10.3390/rs10040641>.
- Mathieu, R., Pouget, M., Cerville, B., Escadafal, R., 1998. Relationships between satellite-based radiometric indices simulated using laboratory reflectance data and typical soil color of an arid environment. *Remote Sens. Environ.* 66, 17–28. [https://doi.org/10.1016/S0034-4257\(98\)00030-3](https://doi.org/10.1016/S0034-4257(98)00030-3).

- McKinnon, T., Hoff, P., 2017. Comparing RGB-Based Vegetation Indices with NDVI for Drone Based Agricultural Sensing. *Agrobotix*, Boulder.
- Micheletti, N., 2015. Structure from motion (SfM) photogrammetry. In: Clarke, L.E., Nield, J. (Eds.), *Geomorphol. Tech.* British Society for Geomorphology.
- OSMRE, 2015. Remote Sensing Pilot Project A Study in the Use of High Resolution Satellite Imagery to Assist with Coal Mine Inspections in Support of the Surface Mining Control and Reclamation Act of 1977.
- Osterkamp, W.R., Joseph, W.L., 2000. Climatic and hydrologic factors associated with reclamation. *Am. Soc. Agron.* 41, 192–215. <https://doi.org/10.2134/agronmonogr41.c8>.
- Padró, J.C., Carabassa, V., Balagué, J., Brotons, L., Alcañiz, J.M., Pons, X., 2019. Monitoring opencast mine restorations using Unmanned Aerial System (UAS) imagery. *Sci. Total Environ.* 657, 1602–1614. <https://doi.org/10.1016/j.scitotenv.2018.12.156>.
- Pons, X., 2004. Centre de Recerca Ecològica i Aplicacions Forestals, CREAM. *MiraMon. Sistema d'Informació Geogràfica i software de Teledetecció*, Bellaterra.
- Pons, X., 2019. *MiraMon. Sistema d'Informació Geogràfica i software de Teledetecció. Versió 8.1j*. Centre de Recerca Ecològica i Aplicacions Forestals, CREAM. Bellaterra, ISBN 84-931323-4-9. <http://www.creaf.uab.cat/miramon/>.
- Pix4D, 2017. *USER MANUAL Pix4Dmapper 4*, 305, 1.
- QGIS Development Team, 2020. QGIS geographic information system. Open Source Geospatial Foundation. <http://qgis.org>.
- Rouse, R.W.H., Haas, J.A.W., Deering, D.W., 1974. Monitoring vegetation systems in the great Plains with ERTS. *Third Earth Resour. Technol. Satell. Symp. I. Tech. Present.* NASA SP-351 309–317.
- Ruiz-Carulla, R., Corominas, J., Hürlimann, M., 2017. Experiencias Con drones Para El Estudio de Movimientos de Ladera. *Cimne* 1–12.
- Tarolli, P., Sofia, G., 2016. Human topographic signatures and derived geomorphic processes across landscapes. *Geomorphology* 255, 140–161. <https://doi.org/10.1016/j.geomorph.2015.12.007>.
- Tucker, C.J., 1979. Red and photographic infrared linear combinations for monitoring vegetation. *Remote Sens. Environ.* [https://doi.org/10.1016/0034-4257\(79\)90013-0](https://doi.org/10.1016/0034-4257(79)90013-0).
- Vidal, O., Goffé, B., Arndt, N., 2013. Metals for a low-carbon society. *Nat. Geosci.* 6, 894–896. <https://doi.org/10.1038/ngeo1993>.
- Vidal-Macua, J.J., Nicolau, J.M., Vicente, E., Moreno-de las Heras, M., 2020. Assessing vegetation recovery in reclaimed opencast mines of the Teruel coalfield (Spain) using Landsat time series and boosted regression trees. *Sci. Total Environ.* 717, 137250. <https://doi.org/10.1016/j.scitotenv.2020.137250>.
- Wu, C., 2013. Towards Linear-time Incremental structure from motion. In: *Proceedings - 2013 International Conference on 3D Vision, 3DV 2013*. <https://doi.org/10.1109/3DV.2013.25>.
- Xiang, J., Chen, J., Sofia, G., Tian, Y., Tarolli, P., 2018. Open-pit mine geomorphic changes analysis using multi-temporal UAV survey. *Environ. Earth Sci.* 77 <https://doi.org/10.1007/s12665-018-7383-9>.
- Zhang, X., Zhang, F., Qi, Y., Deng, L., Wang, X., Yang, S., 2019. New research methods for vegetation information extraction based on visible light remote sensing images from an unmanned aerial vehicle (UAV). *Int. J. Appl. Earth Obs. Geoinf.* 78, 215–226. <https://doi.org/10.1016/j.jag.2019.01.001>.
- Parrot Drones SAS, 2016. *Parrot Sequoia - Users Manual*.